Available online at www.sciencedirect.com

SCIENCE DIRECT®

Polyhedron 23 (2004) 1777–1784

POLYHEDRON

www.elsevier.com/locate/poly

Perhalogenated porphyrinic derivatives with indium and thallium: the X-ray structures of (β-Cl_4TPP)Tl(Cl), (β-Cl_4TPP)In(Cl) and (T*p*FTPP)Tl(Cl) ☆

Catherina Raptopoulou [a], Dimitra Daphnomili [b], Athanassios Karamalides [c], Massimo Di Vaira [c], Aris Terzis [a], Athanassios G. Coutsolelos [b,*]

[a] *NCRS, Demokritos, Agia Paraskevi, 15310 Athens, Greece*
[b] *Laboratory of Bioinorganic Coordination Chemistry, Department of Chemistry, School of Sciences, University of Crete, P.O. Box 1470, 71409 Heraklion Crete, Greece*
[c] *Universita degli Studi di Firenze, Dipartimento di Chimica, Via della Lastruccia 5, Sesto Fiorentino, Firenze, Italy*

Received 10 November 2003; accepted 24 March 2004
Available online 10 May 2004

Abstract

The synthesis and spectroscopic characterization of new substituted porphyrinate complexes are reported. The investigated compounds are represented by the formula (Porph)M(Cl) where Porph are T*p*FPP, TPyP, β-Cl_4TPP, β-Cl_8TPP or β-Cl_4TPP, and M = In or Tl.

UV–Vis and NMR spectroscopies of the title complexes confirm the proposed molecular formula and are described extracting all plausible information. The study is completed by three X-ray structures of (β-Cl_4TPP)Tl(Cl), (β-Cl_4TPP)In(Cl) and (T*p*FTPP)Tl(Cl).

Compounds (β-Cl_4TPP)Tl(Cl) and (β-Cl_4TPP)In(Cl) are isostructural and they were treated in a similar way. The chloride substituents on the porphyrin core were found to be disordered in both compounds and they were refined anisotropically with occupation factors free to vary. The porphyrin core is saddle distorted while there is no twist distortion as judged by the large values of the dihedral angles formed between the phenyl rings and the $C_{20}N_4$ mean plane. In compound (T*p*FTPP)In(Cl), the dihedral angles between the pentafluorophenyl rings and $C_{20}N_4$ are very close to the ideal value of 90°.

Keywords: Metalloporphyrins; Indium; Thallium

1. Introduction

Porphyrin complexes of the main group III_B are ideal model compounds since they show considerable flexibility of the core geometries depending on the peripheral substitution and on axial ligation [1–9].

Meso-substitution as well as β-halogenation on the porphyrin core is expected to alter their spectroelectrochemical properties. Investigations have been carried out to probe the electronic structures of these systems by different approaches involving spectral and redox potential data as well as semi-empirical calculations. For β-halogenated porphyrins with more than four halogens, the electronic effects of the peripheral substituents causes a decrease of the basicity of the porphyrin ring, a red shift of the Soret band transition energy and a decrease in HOMO–LUMO energy gap [10–18].

Metal ions incorporated into perhalogenated complexes are mainly copper, zinc and nickel [10,12,14,16–18] as far as concerns the four coordinated ions, while iron complexes have also been reported due to the enhanced catalytic activity of these systems [11,18,19].

☆ Supplementary data associated with this article can be found, in the online version, at doi:10.1016/j.poly.2004.04.010.

* Corresponding author. Tel.: +30-2810-393636; fax: +30-2810-393601.

E-mail address: coutsole@chemistry.uoc.gr (A.G. Coutsolelos).

0277-5387/\$ - see front matter © 2004 Elsevier Ltd. All rights reserved.
doi:10.1016/j.poly.2004.04.010

Recently the X-ray study of a lanthanide perhalogenated complex has been published [14]. It has been suggested that the metal ion and its environment influence the redox potential of these systems.

Based on a recently published procedure [14] we achieved the synthesis of halogenated In(III) and Tl(III) complexes. Their physicochemical features are compared with those of *meso*-substituted derivatives. Metallation with In or Tl offers a unique probe to study the influence of peripheral substituents and/or of the central metal on their physicochemical properties. A work correlating the ^{205}Tl NMR chemical shifts to the basicity of the ring, the axial ligation and the oxidation state has already been published by our group [20]. Monomeric thallium complexes provide ^{205}Tl signals from approximately 2850–2700 ppm following a decreasing order of basicity, while in the case of dimeric complexes (with a Rh:→Tl metal bond, typical +1 oxidation state of Tl) the signal is shifted more than 2000 ppm to the region of 180–200 ppm [21].

Finally, part of our research interest is the formation of single metal–metal bonded porphyrinic complexes. Monomeric metalloporphyrins of In or Tl are excellent precursors for the synthesis of new metal–metal bonded dimers. The nature of the monomeric complexes is expected to influence dramatically the properties of the formed dimers.

2. Experimental

2.1. Materials

All chemical were reagent grade and were used without further purification except as noted. Basic type I alumina was activated at 150 °C for at least 24 h.

2.2. Syntheses

The synthesis of free bases followed previously published procedures [14,22]. The preparation of thallium(III) complexes was based on Abraham's method [23]. The preparation of In complexes was based on the "acetate method" [24].

2.2.1. Syntheses of (Porph)Tl–Cl complexes

(T*p*FPP)TlCl (**1**): 0.1 mmol of (T*p*FPP)H_2 and 1 mmol of $Tl^{III}(CH_3COO)_3 \times 11/2H_2O$ were dissolved in 100 ml THF. The reaction mixture was refluxed for 24 h. After cooling, THF was removed and the solid residue was dissolved in CH_2Cl_2 and washed with a saturated aqueous solution of NaCl. Chromatographic separation of the crude product was performed on a SiO_2 column (4 cm × 3 cm). The metallated product was eluted with CH_2Cl_2/C_6H_{14} (4/6 v/v) as eluents (yield: 60%).

(TPyP)TlCl (**2**): The same reaction process as mentioned above was followed. The product was recovered after recrystallization from a mixture of CH_2Cl_2/C_6H_{14} (1/3 v/v), (yield: 94%).

(β-Cl_4TPP)TlCl (**3**): The reaction was performed as for compound **1**. A column of SiO_2 (4 cm × 3 cm) was used for the chromatographic separation. The desired product was eluted with CH_3OH/CH_2Cl_2 (50/50 v/v-20/80 v/v) as eluents, (yield: 65%).

(β-Br_4TPP)TlCl (**4**): The preparation of the crude product was the same as described above. The column separation was performed on SiO_2 (4 cm × 3 cm). The desired metalloporphyrin derivative was eluted with CH_2Cl_2, (yield: 67%).

(β-Cl_8TPP)TlCl (**5**): The reaction conditions mentioned before were also followed for the synthesis of the crude product **5**. The chromatographic separation was performed on SiO_2 column (6 cm × 4 cm). The product was eluted with toluene/hexane (8/2 v/v), (yield: 60%).

2.2.2. Syntheses of (Porph)In–Cl complexes

(T*p*FPP)InCl (**6**): 0.15 mmol of (T*p*FPP)H_2, 1.5 mmol of $InCl_3$ and 16 mmol of CH_3COONa were dissolved in 50 ml of glacial acetic acid. The reaction mixture was refluxed for 24 h. The solvent was removed under reduced pressure and the solid residue was dissolved in CH_2Cl_2. The solution was extracted from an aqueous solution of $NaHCO_3$ (5% w/v). The organic phase was washed two times with a saturated aqueous solution of NaCl and dried over $MgSO_4$. The solvent was removed and the solid residue was purified. A chromatographic separation was performed on SiO_2 (6 cm × 3 cm). With CH_2Cl_2/hexane (4/6 v/v) the free base was eluted. Increasing gradually the polarity of the solvents to CH_2Cl_2/hexane (8/2 v/v) the metalloporphyrin was eluted, (yield: 85%).

(TPyP)InCl (**7**): The previous synthetic route was also performed for compound **7**. Basic Al_2O_3 (5 cm × 3 cm) (Grade 1) was used in order to perform the chromatographic separation. With CH_2Cl_2/MeOH (200/5 v/v) the desired product was collected, (yield: 87%).

(β-Cl_4TPP)InCl (**8**): The preparation followed the previously described method for complex **6**. The chromatographic separation was performed on basic Al_2O_3 (5 cm × 3 cm) (Grade 1). The metalloporphyrin was eluted with a mixture of CH_2Cl_2/MeOH (7/3 v/v), (yield: 70%).

(β-Br_4TPP)InCl (**9**): The preparation was the same as described above. The crude product was chromatographed on SiO_2 (5 cm × 4 cm). The elution of the metallated porphyrin was achieved with toluene, (yield: 60%).

(β-Cl_8TPP)InCl (**10**): The reaction conditions were the same but with THF as reaction solvent due to low solubility of (β-Cl_8TPP)H_2 in the glacial acetic acid. The chromatographic separation was achieved on SiO_2 (6 cm × 4 cm) and the product was eluted with CH_2Cl_2, (yield: 70%).

3. Instrumentation and methods

^1H NMR and ^{13}C NMR spectra were recorded on a Bruker AMX-500 MHz NMR spectrometer using chloroform-D_3 as a solvent. Resonances in the ^1H NMR were referenced versus the residual proton signal of the solvent.

Absorption spectra were collected on a Perkin–Elmer Lamda 6 grating spectrophotometer.

Crystals suitable for X-ray diffraction were obtained by slow evaporation of a saturated toluene solution for compounds **3** and **8** and of a saturated solution of a mixture of 1:1 $CHCl_3$/toluene for compound **6**.

3.1. Data collection and X-ray crystal structure determination

A single crystal with approximate dimensions 0.20 × 0.20 × 0.50 mm for **3,** and 0.10 × 0.10 × 0.30 mm for **8** were mounted in air. Diffraction measurements for **3** and **8** were made on a Crystal Logic Dual Goniometer diffractometer using graphite monochromated Mo Kα radiation. Unit cell dimensions were determined and refined by using the angular settings of 25 automatically centred reflections in the range $1° < 2\theta < 23°$. Intensity data were recorded using $\theta - 2\theta$ scans. Three standard reflections were monitored every 97 reflections over the course of data collection and showed less than 3% variation and no decay. Lorentz polarization and ψ-scan absorption corrections were applied using Crystal Logic software. The structures of **3** and **8** were solved by direct methods using SHELXS-86 [25] and refined by full-matrix least-squares techniques on F^2 with SHELXL-93 [26].

A single crystal of **6**, with approximate dimensions 0.20 × 0.40 × 0.60 mm, was mounted in air on a Siemens-Bruker P4 diffractometer equipped with a rotating anode generator, graphite-monochromated Cu Kα radiation being used for all operations. Cell dimensions were determined from the angular settings of 30 reflections with $32° < \theta < 55°$. Intensity data were recorded by ω–2θ scans and three standards monitored every 90 min revealed an overall 14% intensity decay, which was accounted for at data reduction time. A ψ-scan absorption correction was applied. Structure solution and refinement were performed with SHELX [25,26].

A summary of crystallographic data for **3**, **6** and **8** is given in Table 1.

Compounds **3** and **8** are isostructural and they were treated in a similar way. The chloride substituents on the porphyrin core were found disordered in both **3** and **8** and they were refined anisotropically with occupation factors free to vary. The chlorine substitution on the

Table 1
Summary of crystal, intensity collection and refinement data for compounds (β-Cl_4TPP)TlCl (**3**), (T*p*FPP)InCl (**6**) and (β-Cl_4TPP)InCl **(8)**

Parameters	(**3**) · $C_6H_5CH_3$	(**8**) · $C_6H_5CH_3$	(**6**) · 1.5(C_6H_6)
Formula	$C_{51}H_{32}Cl_5N_4Tl$	$C_{51}H_{32}Cl_5InN_4$	$C_{53}H_{17}ClF_{20}InN_4$
Fw	1082.43	992.88	1239.98
Crystal system	triclinic	triclinic	monoclinic
Space group	$P\bar{1}$	$P\bar{1}$	$P2_1/n$
Temperature (K)	298	298	298
Unit cell dimensions			
a (Å)	13.942(6)	13.914(6)	14.775(3)
b (Å)	14.284(6)	14.198(7)	12.979(2)
c (Å)	13.368(6)	13.238(6)	26.222(6)
α (°)	105.32(1)	104.73(1)	–
β (°)	118.44(1)	118.02(1)	92.66(2)
γ (°)	90.39(1)	91.10(1)	–
V (Å^3)	2230(2)	2203(2)	5023(2)
Z	2	2	4
ρ_{calcd} (g cm^{-3})	1.612/1.60	1.497/1.48	1.640/1.63
Radiation, θ (Å)	Mo Kα 0.71073	Mo Kα 0.71073	Cu Kα 1.5418
μ (mm^{-1})	3.962	0.881	5.309
Reflections collected/unique [R_{int}]	7783/7428 [0.0156]	6412/6110 [0.0237]	9238/5827 [0.0388]
Data with $I > 2\sigma(I)$	6340	4345	5618
Parameters refined	561	562	758
$(\Delta\rho)_{max}$, $(\Delta\rho)_{min}$ (e Å^{-3})	0.696/−0.794	0.705/−0.521	1.998/−0.715
w[a]	$a = 0.0657$, $b = 1.2315$	$a = 0.0703$, $b = 9.0137$	$a = 0.0921$, $b = 9.6349$
Goodness-of-fit (on F^2)	1.179	1.014	1.134
R_1[b], wR_2[c] (all data)	0.0595, 0.1260	0.1004, 0.1984	0.0584, 0.1618
R_1[b], wR_2[c] ($I > 2\sigma(I)$)	0.0469, 0.1184	0.0680, 0.1625	0.0573, 0.1606

[a] $w = 1/[\sigma^2(F_o^2) + (aP)^2 + bP]$ and $P = (\max(F_o^2, 0) + 2F_c^2)/3$.
[b] $R_1 = \sum(|F_o| - |F_c|)/\sum(|F_o|)$.
[c] $wR_2 = \{\sum[w(F_o^2 - F_c^2)^2]/\sum[w(F_o^2)^2]\}^{1/2}$.

pyrroles of the porphyrin skeleton is unsymmetrical in both **3** and **8**. The distribution of the chloride ions is unsymmetrical because there are two pyrrole rings, which are monosubstituted, one that is doubly substituted and one unsubstituted. In compound **3,** there is 64% probability of the presence of chlorine substituents in C$_2$, C$_7$, C$_{12}$, C$_{13}$ and 36% probability of the presence of the substituents in the remaining C$_\beta$ atoms of the porphyrin. The corresponding probabilities in compound **8** are 60% in C$_2$, C$_7$, C$_{12}$, C$_{13}$ and 40% in the remaining C$_\beta$ positions. In both **3** and **8**, all the non-hydrogen atoms were refined anisotropically, except those of the toluene solvent molecule, which were refined isotropically. The toluene molecule was found disordered over two orientations and was refined with occupation factors of a total sum of one. All H atoms were introduced at calculated positions as riding on bonded atoms; no H atoms for the toluene solvent molecule were included in the refinement.

In the model for the structure of **6** all the non-hydrogen atoms were refined anisotropically and the hydrogen atoms, both of the TPP ring and of the solvent molecules, were in calculated positions, riding. Presence of solvate molecules in the structure was modelled by two benzene molecules: one was distributed over two orientations whose complementary occupancy factors were refined and the other one, lying in proximity of an inversion centre, was assigned a fixed 0.50 occupancy factor value.

4. Results and discussion

4.1. NMR

The title complexes are fully characterized by ^{1}H NMR and ^{13}C NMR, while for the case of pentafluoroporphyrins ^{19}F NMR experiments were performed.

By the performance of ^{1}H NMR we observed the characteristic differentiation of *ortho*- and *ortho′*-protons. There is only one exception for the case of octahalogenated complexes (Table 2). In the case of Tl complexes a scalar coupling of pyrrolic protons with the Tl nucleus is observed, which is measured close to 75 Hz.

Taking advantage of the 100% natural abundance of spin 1/2 ^{19}F and its high gyromagnetic ratio, ^{19}F NMR experiments were performed. Five separate signals were observed (Table 3). The porphyrin ring current and the position of the fluorine atoms related to the porphyrin ring differentiate them. The furthest downfield signals, which appeared as two doublets, are attributed to *ortho*-F and to ortho′-F ($J = 23.5$ Hz). The fluorine atom at the *para* position appeared as a triplet. Metallation mainly effects the chemical shifts of *ortho*-F, *ortho′*-F and *meta*-F compared to the free base [27].

^{13}C- NMR signals spread in a 200 ppm region (Table 4). Assignment was based on heteronuclear experiments (HMQC, HMBC). We can distinguish two major groups for carbon frequencies. The aromatic carbons resonate between 130 and 170 ppm and the methinic carbons in the region of 90–120 ppm. The chemical data does not present any unexpected information in respect to other metalloporphyrinic derivatives. However the chemical shifts for C$_{\text{ph}}$ are sensitive to the number of the halogen atoms: 140.18 ppm for (β-Cl$_4$TPP)TlCl to 144.2 ppm for (β-Cl$_8$TPP)TlCl.

C$_\beta$ are the most sensitive carbon atoms to substitution. For tetrahalogenated complexes C$_\beta$ provide two signals, one which is attributed to C$_\beta$-H and one to C$_\beta$-X (X = Cl, Br). In the case of (β-Cl$_4$TPP)TlCl, C$_\beta$–Cl resonate at 135.34 ppm. The signal at 133.72 ppm was assigned through heteronuclear experiments to C$_\beta$-H and for the tetrabrominated analogue at 134.2 ppm. In the case of octahalogenated complexes C$_\beta$–Cl is dishielded at 137.86 ppm for (β-Cl$_8$TPP)TlCl.

4.2. UV–visible spectroscopy

The position (β-pyrrole or *meso*) of the substitution is the factor which affects more or less in each case the spectrochemical properties of the macrocycle (Table 5).

Table 2
^{1}H NMR chemical shifts of complexes (Porph)In$^{\text{III}}$Cl and (Porph)Tl$^{\text{III}}$Cl in CDCl$_3$

Complex	*para*-H (*p*-H)	*meta*-H (*m*-H)	*ortho*-H (*o*-H)	*ortho*-H′ (*o*′-H)	pyr-H
(T*p*FPP)TlCl **(1)**					9.14 ($J = 61$)[a]
(TPyP)TlCl **(2)**		9.11 (d)	8.37	8.10	9.13 ($J = 63.3$)[a]
(β-Cl$_4$TPP)TlCl **(3)**	7.84 (m)	7.75 (m)	8.14 (d)	8.03 (d)	8.89
(β-Br$_4$TPP)TlCl **(4)**	7.84 (tr)	7.73 (m)	8.14 (m)	8.04 (m)	8.97 ($J = 75$)[a]
(β-Cl$_8$TPP)TlCl **(5)**	7.86 (tr)	7.79 (br)	8.16 (br)	8.16 (br)	
(T*p*FPP)InCl **(6)**					9.15
(TPyP)InCl **(7)**		9.13 (d)	8.37	8.10	9.14
(β-Cl$_4$TPP)InCl **(8)**	7.83 (tr)	7.77 (m)	8.15 (m)	7.98 (m)	8.92
(β-Br$_4$TPP)InCl **(9)**	7.85 (tr)	7.77 (m)	8.15 (m)	8.01 (m)	8.95
(β-Cl$_8$TPP)InCl **(10)**	7.86 (tr)	7.79 (s,br)	8.15 (s,br)	8.15 (s,br)	

δ in ppm.

[a] In parenthesis ^{205}Tl–H coupling in Hz.

Table 3
^{19}F NMR data for (T*p*FPP)M^{III}Cl (M = In, Tl) complexes in CDCl$_3$

	ortho-F (*o*-F)	ortho′-F (*o*′-F)	meta-F (*m*-F)	meta′-F (*m*′-F)	para-F (*p*-F)
(T*p*FPP)H$_2$[a]	−136.92	−136.92	−161.81	−161.81	−151.70
(T*p*FPP)In^{III}Cl	−135.66	−137.34	−161.03	−161.6	−150.83
(T*p*FPP)Tl^{III}Cl	−135.84	−137.22	−161.09	−161.56	−150.84

δ in ppm.

[a] Taken from [27].

Table 4
^{13}C NMR data of (β-X$_n$TPP)In^{III}Cl and (β-X$_n$TPP)Tl^{III}Cl(X = Cl or Br $n = 4$ or 8) in CDCl$_3$

	C$_o$	C$_{o'}$	C$_{meta}$	C$_{meta'}$	C$_{para}$	C$_{ph}$	C$_{meso}$	C$_a$	C$_\beta$
(Cl$_4$TPP)TlCl	134.57	135.02	127.67	127.48	129.96	140.18	122.65	151.98	133.79 129.65
(Br$_4$TPP)TlCl	134.48	135.17	127.48	127.79	129.24	141.20	123.12	151.97	133.86
(Cl$_8$TPP)TlCl	135.80	135.44	128.64	128.41	130.15	144.20	122.8		137.86
(Cl$_4$TPP)InCl	134.56	134.73	127.56	127.37	129.04	140.60	121.55	150.03	133.72 135.34
(Br$_4$TPP)InCl	134.44	135.06	127.78	127.46	129.21	140.07	122.10	150.65	134.22
(Cl$_8$TPP)InCl	135.83	135.27	128.51	128.51	130.10	143.15	121.63		137.8

δ in ppm.

Table 5
UV–visible data of (Porph)In^{III}Cl and (Porph)Tl^{III}Cl complexes in toluene

	B bands			*Q(2,0)*	*Q(1,0)* or β	*Q(0,0)* or α	β/α
(T*p*FPP)TlCl (**1**)		412 *(4.63)*	433 *(5.70)*	523 *(3.48)*	563 *(4.38)*	596 *(3.25)*	1.35
(TPyP)TlCl (**2**)		413 *(4.53)*	434 *(5.66)*	526 *(3.41)*	565 *(4.29)*	604 *(3.77)*	1.14
(β-Cl$_4$TPP)TlCl (**3**)	359 *(4.33)*	422 *(4.57)*	443 *(5.47)*	535 *(3.46)*	575 *(4.14)*	614 *(3.79)*	1.09
(β-Br$_4$TPP)TlCl (**4**)	363 *(4.18)*	424 *(4.63)*	446 *(5.58)*	539 *(3.59)*	576 *(4.26)*	617 *(3.920)*	1.09
(β-Cl$_8$TPP)TlCl (**5**)	393 *(4.52)*		468 *(5.35)*	565	604 *(3.98)*	660 *(4.04)*	0.98
(T*p*FPP)InCl (**6**)		403 (4.66)	425 (5.63)	516 (3.40)	556 (4.38)	591 (3.34)	1.31
(TPyP)InCl (**7**)	330 (4.28)	405 (4.58)	426 (5.79)	520 (3.51)	559 (4.35)	597 (3,72)	1.17
(β-Cl$_4$TPP)InCl (**8**)	352 (4.31)	412 (4.60)	435 (5.61)	529 (3.49)	568 (4.27)	607 (3.81)	1.12
(β-Br$_4$TPP)InCl (**9**)	358 (4.36)	416 (4.66)	438 (5.64)	532 (3.57)	570 (4.32)	609 (3.90)	1.11
(β-Cl$_8$TPP)InCl (**10**)	387 (4.45)		456 (5.51)	552 (3.54)	591 (4.10)	643 (4.02)	1.02

λ_{max} (nm), $\log\varepsilon$ (dm^{-1} mol^{-1} cm^{-1}).

Theoretical as well as experimental work concerning the tetraphenyl porphyrin has demonstrated that the relative ordering of the a$_{1u}$ and a$_{2u}$ orbitals is particularly sensitive to *meso*-substitution [28]. The a$_{1u}$ orbital localizes electron density predominantly on C$_\alpha$ whereas a$_{2u}$ electron is concentrated on the *meso* position. So, an electron-withdrawing group such as a perfluorophenyl group at the *meso* position is expected to lower the energy of the a$_{2u}$ orbital with respect to a$_{1u}$ [15].

In the case of halogenated complexes semi-empirical AM1 and spectroscopic calculation revealed that both the electronic properties of the halogen and the distortion of the macrocycle results in a reduced HOMO–LUMO energy gap [10,12,14,18,29]. On the other hand theoretical calculations relative to the influence of metal–porphyrin interactions on the energy of the frontier orbital revealed that mainly the a$_{2u}$ orbital sensed the metal perturbation which places considerable electron density on the pyrrole nitrogen, while a$_{1u}$ has nodes through the nitrogen and cannot interact directly with the metal [28c,30].

The porphyrinic complexes **1**, **2**, **6** and **7** which are *meso* substituted possess spectral features of "normal" type porphyrins [31] (Table 5) with no significant shifts of λ_{max} relative to the corresponding tetraphenyl derivatives [2].

Metallation of tetrahalogenated porphyrin results in bathochromically shifted bands. The intensity of the α band increases relative to the tetraphenyl complexes of In and Tl. This observation is more pronounced in the case of octahalogenated complexes where the intensity ratio of the molar absorptivities (β/α) is reduced. To a first approximation the β/α value correlates with the stabilization of the central metal [32]. The porphyrin ring with a large β/α value stabilizes the central metal. This is in good agreement with the reduced electron density for the octahalogenated complexes.

The *Soret* band of the octa-halogenated complexes (**5**, **10**) is red shifted relative to the free base, in contrast to the four coordinated complexes which possess blue-shifted *Soret* bands. [10,16]. The difference in $\lambda_{\max}$ of the *Soret* band between octahalogenated complexes **5**, **10** and the *meso* substituted **1**, **2**, **6**, **7** reflect the reduced HOMO–LUMO energy gap expected in view of the ring distortion as well as to the inductive effect of the halogen atoms.

The differences observed concerning the $\lambda_{\max}$ of the *Soret* band for the two series of In and Tl complexes with the same porphyrinic ligand can be attributed to the different electronegativity values of the two metals. More electronegative metals lower the a_{2u} orbital [28c,30b]. In addition, the ionic radii of the two metals play an important role. The size of the ionic radius of Tl (1.05 Å) leads to an out of the Δ_{4N} plane displacement which is larger than that for the In complexes [33] and it is also observed in the present X-ray structures.

4.3. Description of the structures

The molecular structures of compounds **3**, **6** and **8** are shown as ORTEP plots in Figs. 1–3 respectively. Selected bond distances and angles are listed in Table 6, structural characteristics of the porphyrin core of all the three structures are given in Table 7. Compounds **3** and **8** are the corresponding thallium(III) and indium(III) complexes of tetrachloro-tetraphenylporphyrin and are isostructural, so they will be discussed together. In both compounds, the coordination geometry about the metal is square pyramidal with the four nitrogen atoms of the porphyrin defining the equatorial plane and the chloride ion occupying the apical position. The M–N bond distances range from 2.199(6) to 2.220(6) Å for **3** (average value 2.210 Å) and from 2.150(7) to 2.163(7) Å for **8** (average value 2.158 Å). The M–Cl bond lengths are 2.442(2) and 2.367(3) Å for **3** and **8** respectively. The metal ion lies 0.70 and 0.58 Å in **3** and **8** respectively, out of the equatorial plane of the square pyramid toward the axial chloride ligand. The presence of the metal ions along with the substitution on the C_β and C_m atoms of the porphyrin results in the distortion of the porphyrin core. The presence of the chlorine atoms on C_β carbon atoms of the porphyrin skeleton in both **3** and **8** results in the saddling distortion of the ligand, expressed by the mean absolute displacement of the C_β atoms from the $C_{20}N_4$ mean plane (0.39 Å for C_2, C_7, C_{12}, C_{13} in both **3** and **8**).

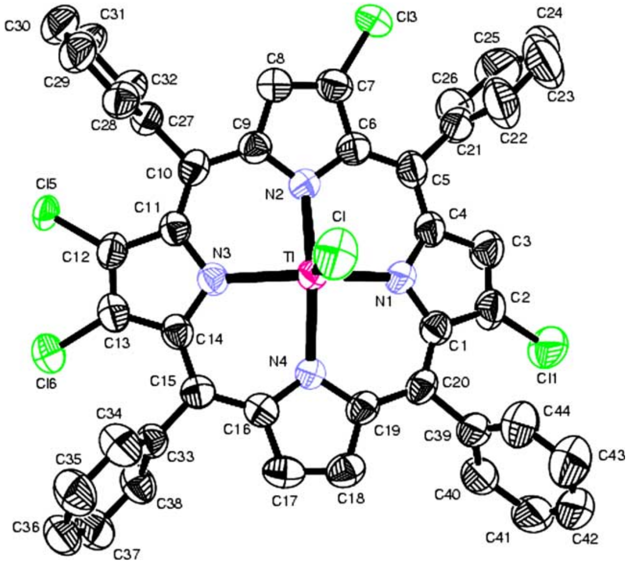

Fig. 1. ORTEP plot of (β-Cl_4TPP)TlCl (**3**).

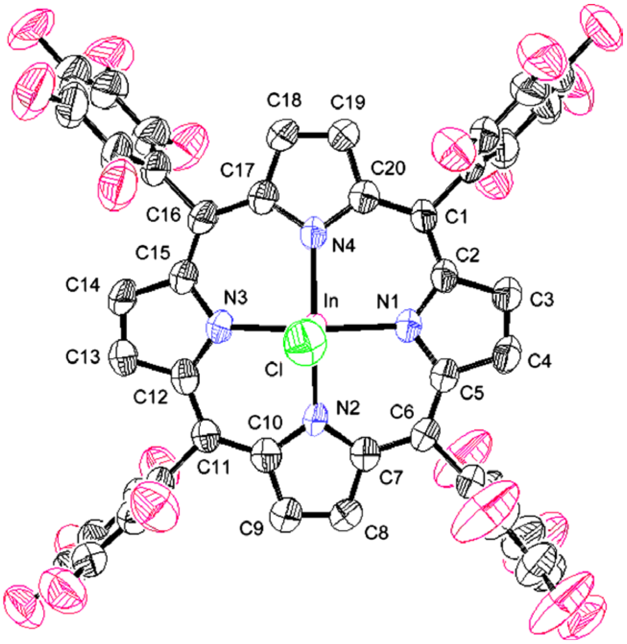

Fig. 2. ORTEP plot of (T*p*FPP)InCl (**6**).

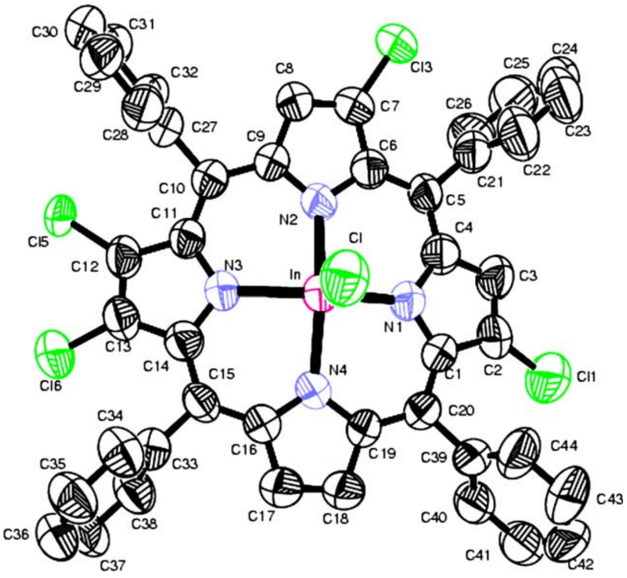

Fig. 3. ORTEP plots of (β-Cl_4TPP)InCl (**8**).

Table 6
Selected bond distances (Å), angles (°), and averages for (β-Cl_4TPP)TlCl · $C_6H_5CH_3$ (**3**), (β-Cl_4TPP)TlCl · $C_6H_5CH_3$ (**8**) and (T*p*FPP)InCl · 1.5(C_6H_6) (**6**)

	3 · $C_6H_5CH_3$	**8** · $C_6H_5CH_3$	**6** · 1.5(C_6H_6)
Bond distances			
M–Cl	2.442(2)	2.367(3)	2.360(2)
M–N(1)	2.212(6)	2.162(7)	2.154(5)
M–N(2)	2.207(6)	2.150(7)	2.141(5)
M–N(3)	2.199(6)	2.163(7)	2.161(5)
M–N(4)	2.220(6)	2.156(7)	2.135(5)
N–C_α	1.376	1.375	1.367
C_α–C_β	1.453	1.446	1.442
X–C_β	1.691[a]	1.674[b]	–
C_α–C_m	1.410	1.403	1.398
C_m–C_{phenyl}	1.484	1.494	1.505
Bond lengths			
$(N–M–N)_{cis}$	84.2	85.9	86.2
$(N–M–N)_{trans}$	142.9	149.0	149.9
$(Cl–M–N)_{axial}$	108.6	105.5	105.0
C_α–N–C_α	109.2	108.7	108.1
N–C_α–C_β	107.6	107.7	108.3
C_α–C_β–C_β	107.8	107.9	107.6
N–C_α–C_m	126.3	125.8	125.7

[a] For Cl(1), Cl(3), Cl(5) and Cl(6) with occupancy 64%.
[b] For Cl(1), Cl(3), Cl(5) and Cl(6) with occupancy 60% (see text for details).

Table 7
Structural characteristics of the compounds (β–Cl_4TPP)Tl–Cl · $C_6H_5CH_3$ (**3**), (β–Cl_4TPP)Tl–Cl · $C_6H_5CH_3$ (**8**) and (T*p*FPP)In–Cl · 1.5(C_6H_6) (**6**) indicating the distortion of the porphyrin core

Atom(s)	**3** · $C_6H_5CH_3$	**8** · $C_6H_5CH_3$	**6** · 1.5(C_6H_6)
N	0.017	0.031	0.074
C_m	0.081	0.094	0.061
C_β	0.387[a]	0.391[a]	0.097[b], 0.101[c]
Cl1	0.689[d]	0.689[d]	–

Dihedral angles with the $C_{20}N_4$ mean plane

Group	**3** · $C_6H_5CH_3$	**8** · $C_6H_5CH_3$	**6** · 1.5(C_6H_6)
Pyrroles	12.69, 9.97	12.33, 9.56	4.16, 5.00
	10.85, 9.21	10.85, 8.43	3.33, 7.28
Phenyls	76.71, 72.74	76.66, 72.41	74.96, 89.58
	66.70, 65.10	67.55, 64.12	87.23, 73.55

Average absolute displacement of selected atoms of the porphyrin from the $C_{20}N_4$ mean plane.
[a] Average absolute value of C(2), C(7), C(12) and C(13) displacements.
[b] Average absolute value of C(3), C(8), C(13) and C(18) displacements.
[c] Average absolute value of C(4), C(9), C(14) and C(19) displacements.
[d] Average absolute value of Cl(1), Cl(3), Cl(5) and Cl(6) displacements.

The average absolute displacement of the corresponding chlorine atoms bonded to C_β atoms is 0.69 Å (for Cl_1, Cl_3, Cl_5, Cl_6 in both **3** and **8**). On the other hand, the average absolute displacement of the C_m atoms from the porphyrin core (0.081 and 0.094 Å in **3** and **8** respectively) along with the rather large values of the dihedral angles formed between the phenyl rings and the $C_{20}N_4$ mean plane (65.10°–76.71° and 64.12°–76.66° in **3** and **8** respectively) indicate that there is no twist distortion of the porphyrin skeleton. The pyrrole rings are planar within experimental error and they are tilted alternatively up and down with respect to the porphyrin core mean plane by 9.21°–12.69° in **3** and 8.43°–12.33° in **8**.

In compound **6**, the nitrogen atoms of the tetra-(pentafluorophenyl)porphyrin define the equatorial plane of the square pyramidal geometry about the indium(III) ion while the apical position is occupied by the chloride ion. The metal ion lies 0.63 Å out of the equatorial plane towards the axial ligand. The In–N bond distances range from 2.135(5) to 2.161(5) Å (average value 2.148 Å), and the In–Cl bond length is 2.360(2) Å. The lack of substitution on the C_β atoms of the porphyrin skeleton is reflected in the small average absolute displacement of these atoms from the $C_{20}N_4$ mean plane (0.097 and 0.101 Å for C_3, C_8, C_{13}, C_{18} and C_4, C_9, C_{14}, C_{19} respectively) and the small dihedral angles formed between the pyrrole rings and the $C_{20}N_4$ mean plane (3.33°–7.28°). The average absolute displacement of the C_m atoms is also very small (0.061 Å for C_1, C_6, C_{11}, C_{16}) despite the pentafluoro-phenyl substituents. The absence of C_β-substituents in the porphyrin skeleton is also reflected in the large dihedral angles formed between the pentafluoro-phenyl rings and the $C_{20}N_4$ mean plane (73.55°–89.58°) due to the minimization of the steric effects. These values are very close to the ideal value of 90°, which is expected in the non-substituted porphyrins.

5. Concluding remarks

All these complexes could be used as precursors for the synthesis of new metal–metal bonded derivates with

Rh–In or Rh–Tl bonds in order to modify the properties of the metallic bond, stability and/or reactivity. The position of substitution (*β* or *meso*) and the number of halogen atoms (tetra- or octahalogenated complex) impose a pronounced effect on the spectroelectrochemical features of the dimers, which will be discussed in detail in a future article [34].

6. Supplementary data

Crystallographic data for the structural analyses have been deposited with the Cambridge Crystallographic Data Center, CCDC 221431-221333. Copies of this information may be obtained free of charge from The Director, CCDC, 12 Union Road, Cambridge, CB2 1EZ, UK (fax: +44-1223-336033); e-mail: deposit@ccdc.cam.ac.uk or http://www.ccdc.cam.ac.uk.

Acknowledgements

This research was supported by the Greek General Secretariat of Research and Technology, and the ΕΠΕΑΕΚ graduate programs of “Bioinorganic Chemistry” and “Natural Products” through the Special Research Account of the University of Crete.

References

[1] W.R. Scheidt, Y. Lee, J. Struct. Bonding (Berlin) 64 (1987) 1.

[2] A.G. Coutsolelos, A. Tsapara, D. Daphnomili, D.L. Ward, J. Chem. Soc., Dalton Trans. (1991) 3413.

[3] R. Guilard, A. Zrineh, A. Tabard, A. Endo, B. Han, C. Lecomte, M. Souhassou, A. Habbou, M. Ferhat, K.M. Kadish, Inorg. Chem. 29 (1990) 4476.

[4] A. Coutsolelos, R. Guilard, A. Boukhris, C. Lecomte, J. Chem. Soc., Dalton. Trans. (1986) 1779.

[5] A. Boukhris, C. Lecomte, A. Coutsolelos, R. Guilard, J. Organomet. Chem. 29 (1990) 4476.

[6] (a) R. Guilard, S.S. Gerges, A. Tabard, P. Richard, M.A. El Borai, C. Lecomte, J. Am. Chem. Soc. 109 (1987) 7228;
(b) R. Guilard, N. Jagerovic, A. Tabard, P. Richard, L. Courthaudon, A. Louati, C. Lecomte, K.M. Kadish, Inorg. Chem. 30 (1991) 16.

[7] M.O. Senge, K. Ruhlandt-Senge, K.J. Regli, K.M. Smith, J. Chem. Soc., Dalton Trans. (1993) 3519.

[8] L.-F. Chou, Y.-H. Chen, J. Chem. Soc., Dalton Trans. (1996) 3787.

[9] C.-S. Chang, C.-H. Chen, Y.-I. Li, B.-C. Liaou, B.-T. Ko, S. Elango, J.-H. Chen, Inorg. Chem. 40 (2001) 2905.

[10] P. Bhyrappa, V. Krishnan, Inorg. Chem. 30 (2) (1991) 239.

[11] P. Tagliatesta, J. Li, M. Autret, E. Van Caemelbecke, A. Villard, F. D‘ Souza, K.M. Kadish, Inorg. Chem. 35 (1996) 5570.

[12] F. D’ Souza, M.E. Zandler, P. Tagliatesta, Z. Ou, J. Shao, E. Van Caemelbecke, K.M. Kadish, Inorg. Chem. 37 (1998) 4567.

[13] S.G. Di Magno, A.K. Wertsching, C.R. Ros II, J. Am. Chem. Soc. 117 (1995) 8279.

[14] G.A. Spyroulias, A. Despotopoulos, C.P. Raptopoulou, A. Terzis, D. de Montauzon, R. Poilblanc, A.G. Coutsolelos, Inorg. Chem. 41 (2002) 2648, and references cited therein.

[15] P. Ochsenbein, K. Ayougou, D. Mandon, J. Fischer, R. Weiss, R.N. Austin, K. Jayaraj, A. Gold, J. Terner, J. Fajer, Angew. Chem., Int. Ed. Engl. 33 (3) (1994) 348.

[16] J.A. Hodge, M.G. Hill, H.B. Gray, Inorg. Chem. 34 (1995) 809.

[17] D. Mandon, P. Ochsenbein, J. Fischer, R. Weiss, K. Jayaraj, R.N. Austin, A. Gold, P.S. White, O. Brigaud, P. Battioni, D. Mansuy, Inorg. Chem. 31 (1992) 2044.

[18] T. Takeuchi, H.B. Gray, W.A. Goddard III, J. Am. Chem. Soc. 116 (21) (1994) 9730.

[19] P. Ochsenbein, D. Mandon, J. Fischer, R. Weiss, R. Austin, K. Jayaraj, A. Gold, J. Terner, E. Bill, M. Muther, A.X. Trautwein, Ang. Chem., Int. Ed. Engl. 32 (10) (1993) 1437.

[20] A.G. Coutsolelos, D. Daphnomili, Inorg. Chem. 34 (1997) 4614.

[21] D. Daphnomili, W.R. Scheidt, J. Zajicek, A.G. Coutsolelos, Inorg. Chem. 37 (1997) 3675.

[22] (a) J.B. Kim, J.J. Leonard, F.R. Longo, J. Am. Chem. Soc. 11 (1972) 3986;
(b) R.G. Little, J. Abraham, P.A. Loach, J.A. Ibers, J. Heterocycl. Chem. (1975) 343.

[23] R.J. Abraham, G.H. Barnett, K.M. Smith, J. Chem. Soc., Perkin I (1973) 2142.

[24] D. Dolphin, in: The Porphyrins, vol. 4, Academic press, New York, 1979, 197.

[25] G.M. Sheldrick, SHELXS-86: Structure Solving Program, University of Göttingen, Göttingen, Germany, 1986.

[26] G.M. Sheldrick, SHELXL-93: Crystal Structure Refinement, University of Göttingen, Göttingen, Germany, 1993.

[27] E.R. Birnbaum, J.A. Hodge, M.W. Grinstaff, W.P. Schaefer, L. Henling, J.A. Labinger, J.E. Bercaw, H.B. Gray, Inorg. Chem. 34 (1995) 3625.

[28] (a) J. Fajer, D.C. Borg, A. Forman, A.D. Adler, V. Varad, J. Am. Chem. Soc. 96 (1974) 1238;
(b) A.G. Skillman, J.R. Collins, G.H. Loew, J. Am. Chem. Soc. 114 (1992) 9538;
(c) J.A. Shelnutt, V.J. Ortiz, Phys. Chem. 89 (1985) 4733.

[29] (a) P. Bhyrappa, V. Krishnan, Inorg. Chem. (1991) 239;
(b) G. Hariprasad, S. Dahal, B.G. Maiya, J. Chem. Soc., Dalton Trans. (1996) 3429.

[30] (a) M.Z. Zgierski, Chem. Phys. Lett. 124 (1) (1986) 53;
(b) J.A. Shelnutt, J. Phys. Chem. 88 (1984) 4988.

[31] J.W. Buchler, W. Kokisch, P.D. Smith, Struct. Bond. 34 (1987) 79.

[32] J.E. Falk, Porphyrins and Metalloporphyrins, Elsevier, Amsterdam, 1976, p. 34.

[33] (a) R. Guilard, C. Lecomte, K.M. Kadish, Struct. Bond. (1987) 207;
(b) K. Henrick, R.W. Matthews, P.A. Tasker, Inorg. Chem. (1977) 3293;
(c) R.G. Ball, K.M. Lee, A.G. Marshall, J. Trotter, Inorg. Chem. 19 (1980) 1463.

[34] D. Daphnomili, J-H. Agondanou, S. Bénazeth, C. Raptopoulou, A. Terzis, A.G. Coutsolelos, Inorg. Chem. (2004), in press.